ELSEVIER

Chemical Geology 130 (1996) 233–245

CHEMICAL GEOLOGY
INCLUDING
ISOTOPE GEOSCIENCE

A review and analysis of silicate mineral dissolution experiments in natural silicate melts

B.R. Edwards *, J.K. Russell

Department of Geological Sciences, University of British Columbia, Vancouver, B.C. V6T 1Z4, Canada

Received 5 April 1995; accepted 17 November 1995

Abstract

We present a database and a graphical analysis of published experimental results for dissolution rates of olivine, quartz, plagioclase, clinopyroxene, orthopyroxene, spinel, and garnet in basaltic and andesitic melts covering a range of experimental temperatures (1100–1500°C) and pressures (10^5 Pa–3.0 GPa). The published datasets of Donaldson (1985, 1990) and Brearley and Scarfe (1986) are the most complete. Experimental dissolution rates from all datasets are recalculated and normalized to a constant oxygen basis to allow for direct comparison of dissolution rates between different minerals. Dissolution rates (ν) range from $5 \cdot 10^{-10}$ oxygen equivalent moles (o.e.m.) cm^{-2} s^{-1} for olivine in a basaltic melt to $1.3 \cdot 10^{-5}$ o.e.m. cm^{-2} s^{-1} for garnet in a basaltic melt. Values of $\ln \nu$ are Arrhenian for the experiments examined and activation energies range from 118 to 1800 kJ/o.e.m. for quartz and clinopyroxene, respectively.

The relationship between calculated A/RT for the dissolution reactions, where A is the thermodynamic potential affinity, and values of ν is linear for olivine, plagioclase, and quartz. We interpret this as strong evidence in support of using calculated A as a predictor of ν for, at least, superliquidus melt conditions.

1. Introduction

Numerous workers have published experimental results for mineral dissolution in silicate melts (Cooper and Kingery, 1964; Kutolin and Agafonov, 1978; Scarfe et al., 1980; Kuo, 1982; Donaldson, 1985; Kuo and Kirkpatrick, 1985a; Thornber and Huebner, 1985; Brearley and Scarfe, 1986; Zhang et al., 1989; Donaldson, 1990); however, few systematic comparisons of the available data exist (Kuo and Kirkpatrick, 1985b; Brearley and Scarfe, 1986; Edwards and Russell, 1994). Furthermore, none of the published dissolution studies have produced a quantitative predictive model for mineral dissolution rates in silicate melts.

The purpose of this paper is to evaluate and compare the published experimental data for silicate mineral dissolution in naturally occurring silicate melt compositions and to explore the possibility of using calculated affinities (A) for dissolution reactions to predict dissolution rates. We present an analysis of five datasets of experimental measurements for silicate mineral dissolution in natural silicate melts as a function of melt composition, mineral composition, T and P. We summarize the published data, evaluate the consistency of experiments conducted by different workers, and explore the relationships between experimentally determined values of ν

* Corresponding author.

PII S0009-2541(96)00025-3

and melt composition, mineral composition, T, and P. Finally, we investigate the possibility of using calculated values of A to predict experimentally determined values of ν.

2. Methodology

Our current compilation of published mineral dissolution experiments includes data for olivine ($N = 120$), plagioclase ($N = 81$), quartz ($N = 37$), spinel ($N = 24$), clinopyroxene ($N = 25$), orthopyroxene ($N = 18$), and garnet ($N = 10$). Table 1 summarizes the database which includes experiments using natural melt compositions ranging from basalt to rhyolite (Table 2). Excluded from the current database are results from workers who report dissolution rates but do not report the data for individual experiments (e.g., Kutolin and Agafonov, 1978) or experiments using synthetic melt compositions (e.g., Kuo, 1982).

2.1. Evaluation of the datasets

Complete characterization of the experimental conditions and results is important for evaluating the internal consistency of the experiments and is critical for subsequent analysis and modeling. The experimental parameters that need to be reported include: (1) temperature (T); (2) pressure (P); (3) time elapsed between the start and finish of the dissolution experiment (t); (4) initial size and shape of the starting material; (5) final size of the starting material; (6) initial mineral and melt compositions; and (7) estimates of measurement errors. The datasets that best meet the above criteria and therefore form the basis for this analysis are Donaldson (1985, 1990), Thornber and Huebner (1985), Brearley and Scarfe (1986), and Zhang et al. (1989). Results are considered to be internally consistent if all the experiments at the same T and P produce dissolution rates that are within analytical error of each other and vary smoothly and continuously with time.

Multiple experiments at each T and P condition are also important as they serve as checks on the internal consistency of the experiments. In theory values of ν can be calculated on the basis of one experiment; however, such values of ν do not allow any estimation of uncertainty, nor do they allow for assessment of time-dependent vs. time-independent behavior.

Table 1
Summary of silicate mineral dissolution experiments using both natural and synthetic melts (italicized references are used in this work)

Minerals	Number of experiments	Researchers
Olivine	144	Kutolin and Agafonov (1978) [a]; Scarfe et al. (1980) [a]; Kuo (1982) [b]; Marvin and Walker (1985) [b]; *Thornber and Huebner (1985)*; *Donaldson (1985)*; *Brearley and Scarfe (1986)*; *Zhang et al. (1989)*, *Donaldson (1990)*
Orthopyroxene	41	Kutolin and Agafonov (1978) [a]; Scarfe et al. (1980) [a]; Kuo (1982) [b]; *Brearley and Scarfe (1986)*
Clinopyroxene	89	Kutolin and Agafonov (1978) [a]; Scarfe et al. (1980) [a]; Kuo (1982) [b]; *Brearley and Scarfe (1986)*; *Zhang et al. (1989)*
Spinel	25	Scarfe et al. (1980) [a]; *Brearley and Scarfe (1986)*; *Zhang et al. (1989)*
Garnet	17	Kutolin and Agafonov (1978) [a]; Scarfe et al. (1980) [a]; *Brearley and Scarfe (1986)*
Quartz	73	Watson (1982) [a]; Kuo (1982) [b]; *Donaldson (1985)*; *Zhang et al. (1989)*
Alkali feldspar	21	Watson (1982) [a]; Tsuchiyama (1985) [b]
Plagioclase	81	Marvin and Walker (1985) [a]; *Donaldson (1985)*; Tsuchiyama (1985) [b]
Zircon, apatite, rutile	31	Harrison and Watson (1983, 1984); *Zhang et al. (1989)*

[a] Initial sample geometries not reported.
[b] Experiments used synthetic melt compositions.

2.2. Derivation of mineral dissolution rates

Experimental data are reported as changes in dimensions (e.g., radius for spheres) for a given time at one value of T and P. Isothermal dissolution rates (ν) for each mineral are calculated by linear regression assuming an y-intercept of zero; ν is equal to the slope. Fig. 1 illustrates the technique used to calculate ν at each T using dissolution data for olivine ($Fo_{88.5}$) at 1250°C (Donaldson, 1985). The total change in radius of a mineral during each experiment is plotted vs. the time of the experiment. A total of 16 experiments are plotted; only the solid circles are used for the regression because of uncertainties in the final radius for four of the experiments (open circles). The best-fit line for these experiments passes within the estimated measurement uncertainties for all of data points used in the regression.

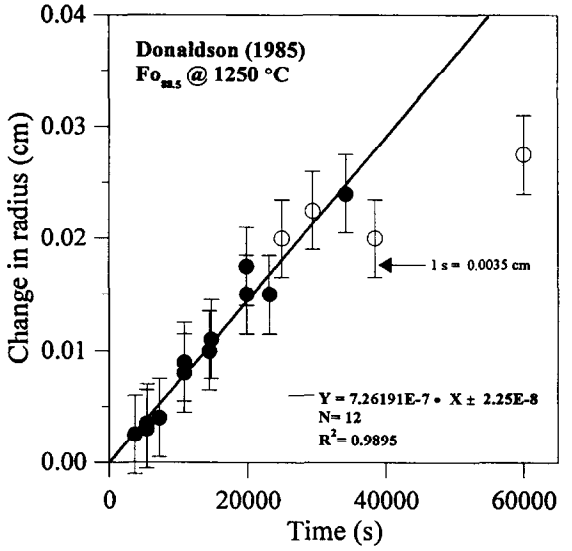

Fig. 1. Experimental data from Donaldson (1985) for olivine ($Fo_{88.5}$) at 1250°C plotted as time (s) vs. change in radius (cm). Data are fit by linear regression to a line with a zero y-intercept; the slope of the fitted line is ν. Experiments in which the entire crystal dissolved (open symbols) were not used in the regression.

2.3. Normalization of experimental data

Direct comparison of experimental mineral dissolution data which derives from different experimental configurations and involves different minerals requires a normalization scheme for two reasons. First, the measured experimental values of ν are dependent on the initial shape of the crystal. For instance, a change in radius of 0.05 cm for a quartz sphere is not necessarily equal to a shortening of a quartz parallelepiped by 0.05 cm in each dimension (Fig. 2). Secondly, a normalization scheme is required to facilitate direct comparison of measured

Table 2
Compositions of melts used in mineral dissolution experiments

Oxides (wt%) Type	Thornber and Huebner (1985) basalt	Thornber and Huebner (1985) Si-enriched basalt	Donaldson (1985; 1990) basalt	Donaldson (1990) andesite	Donaldson (1990) rhyolite	Brearley and Scarfe (1986) basalt	Zhang et al. (1989) andesite
SiO_2	45.09	52.32	51.91	57.7	75.1	48.6	56.5
TiO_2	2.86	2.55	1.16	1.1	0.2	2.20	1.24
Al_2O_3	17.18	16.29	15.85	14.3	14.3	15.6	18.0
Cr_2O_3	na	na	0.06	na	na	na	na
Fe_2O_3	na	na	1.65	na	na	3.13	na
FeO	9.44	8.38	8.27	8.8	0.9	8.53	6.71
MnO	0.02	0.01	0.15	0.2	0.1	0.16	0.13
MgO	10.67	9.09	7.01	6.4	0.2	6.30	3.96
CaO	12.00	9.59	8.66	7.6	0.6	9.85	7.73
Na_2O	1.60	0.67	3.03	2.6	3.9	3.50	3.75
K_2O	0.17	0.19	0.75	0.7	4.5	1.21	1.7
P_2O_5	na	na	0.17	na	na	0.51	0.38
H_2O	na	na	0.86	na	na	0.02	na
Total	99.03	99.09	99.53	99.4	99.8	99.61	100.1

na = not available.

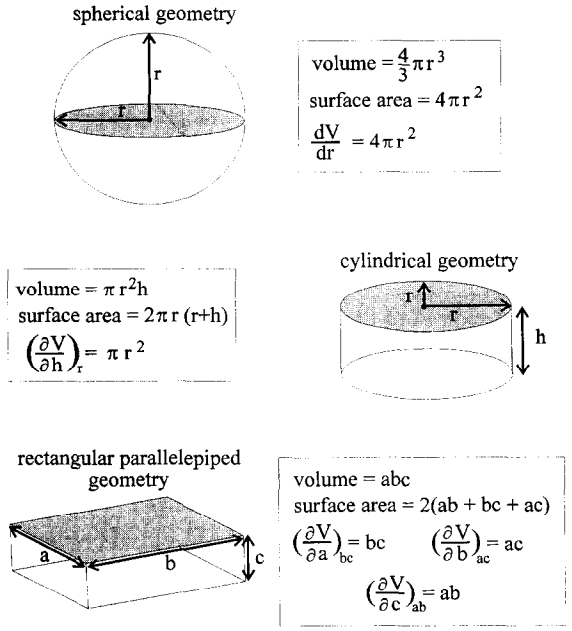

Fig. 2. Mensuration formulas and volume derivatives for geometries of samples used in experiments.

values of ν between minerals that are conventionally modeled with different oxygen numbers (e.g., SiO_2 vs. Mg_2SiO_4).

We use a normalization procedure slightly modified from a method described by Wood and Walther (1983) and Walther and Wood (1984). All regressed ν values are converted from units of cm s^{-1} to oxygen equivalent moles (o.e.m.) cm^{-2} s^{-1} using the procedure outlined below.

(1) We calculate values of ν (cm s^{-1}) by linear regression of isothermal experimental measurements of dr/dt (e.g., Fig. 1).

(2) We normalize values of ν (e.g., Walther and Wood, 1984) using:

$$\nu = \frac{dm}{dt} = \frac{1}{s}\frac{dV}{dr}\frac{dr}{dt} \quad (1)$$

where dm/dt is the normalized dissolution rate (cm s^{-1}), S is the surface area of the dissolving crystal (cm^2), dV/dr is the change in volume with respect to change in radius (cm^3 cm^{-1}), and dr/dt is the measured change in radius over the duration of the experiment (cm s^{-1}). Because different initial mineral geometries have been used by different workers, the dV/dr term and the S term have slightly different formulations depending on starting material geometry (Fig. 2). For spherical geometries (Donaldson, 1985, 1990; Brearley and Scarfe, 1986), the surface area and the volume derivative with respect to changing radius are equal and thus cancel. Zhang et al. (1989) used a cylindrical geometry where only the upper and lower surfaces of the cylinder are exposed to the melt, so the volume derivative with respect to changing thickness and the exposed surface area are equal and also cancel. Thornber and Huebner (1985) used rectangular parallelepiped geometries but only reported changes in one of the three dimensions. For their dataset we assume that changes in all three dimensions are equal, which reduces the combined volume derivative and surface area terms to a constant (0.5). In summary, $dm/dt = dr/dt$ for spherical or cylindrical geometries and $dm/dt = 0.5\ dr/dt$ for rectangular parallelepiped geometries.

(3) We divide the values of ν by the molar volume (V) to convert to units of mol cm^{-2} s^{-1}. Molar volume properties are calculated at experimental T and P conditions using the thermodynamic database and methodology of Berman (1988) and assuming no excess volume of mixing.

(4) Lastly, we multiply the values of ν by the number of oxygens in the mineral formula to get o.e.m. cm^{-2} s^{-1}.

3. Results

3.1. Donaldson (1985, 1990)

Donaldson (1985, 1990) used the same experimental methodology and range of conditions to investigate several different mineral dissolution reactions (Table 3). Donaldson (1985) gives results of 110 dissolution experiments involving quartz normative tholeitic basalt melt (Table 2) and five different mineral compositions (Table 3). Donaldson (1990) ran 26 experiments using three different melt compositions (Table 3) to dissolve spheres of olivine ($Fo_{91.5}$). For both datasets, changes in radius for a given time interval (dr/dt) were determined by measuring initial and final radii of the spheres. Reported measurement errors are ± 0.0035 cm.

The Donaldson (1985, 1990) datasets are the easiest to evaluate for internal consistency because, on average, five experiments were conducted at each set of experimental T and P conditions. The reported values of ν differ slightly from those reported in Table 3 because he does not constrain the regression to pass through the origin. However, this is a necessary constraint because at $t = 0$ the change in radius must also be zero.

3.2. Brearley and Scarfe (1986)

Brearley and Scarfe (1986) used an alkali basalt melt (Table 2) as a solvent for dissolving olivine, clinopyroxene, orthopyroxene, spinel, and garnet over a range of T (1250–1500°C) and P (0.5–3.0 GPa) conditions (Table 4). They used spherical mineral geometries and reported initial and final radii for each experiment. Measurement errors are estimated at ± 0.001 cm for most experiments but are as large as 0.003 cm (10% of the initial diameter of the crystals). They also conducted multiple experiments for each set of isothermal and isobaric conditions save one garnet experiment (Table 4).

Table 3
Summary of dissolution rates at 10^5 Pa extracted from experimental data of Donaldson (1985, 1990)

Mineral	T (°C)	dr/dt (10^{-7} cm s^{-1})	N (number of experiments)	R^2
Quartz	1122	0.1072	2	0.972
	1143	0.2947	5	0.884
	1210	9.636	4	0.991
	1250	13.57	11	0.993
	1300	22.26	5	0.995
Plagioclase (An_{29})	1150	0.2976	1	na
	1210	24.41	4	0.993
	1250	38.38	4	0.996
	1300	65.62	5	0.983
Plagioclase ($An_{52.5}$)	1210	13.18	5	0.923
	1250	29.80	5	0.994
	1300	56.57	5	0.989
Olivine ($Fo_{88.5}$)	1210	0.7645	3	0.912
	1250	7.262	12	0.990
	1300	17.40	2	0.999
Olivine ($Fo_{91.5}$)	1210	2.202	5	0.887
	1250	8.411	10	0.910
	1300	27.54	4	0.997
[a]	1300	27.02	6	0.990
[a]	1300	19.08 [b]	5	0.975
[a]	1300	0.2504 [c]	9	0.972

[a] Donaldson (1990).
[b] Experiments with time > 5 hr were not used.
[c] Experiments with time > 110 hr were not used.

Table 4
Summary of dissolution rates extracted from experimental data of Brearley and Scarfe (1986)

Mineral	T (°C)	P (GPa)	dr/dt (10^{-7} cm s^{-1})	N	R^2
Olivine ($Fo_{89.6}$)	1250	0.5	1.852	3	0.778
	1300	0.5	8.489	3	0.967
	1300	1.2	6.349	3	0.946
	1350	1.2	11.05	3	0.999
	1400	1.2	33.73	13	0.955
	1450	3.0	53.89	5	0.991
	1500	3.0	286.7	2	0.958
Clinopyroxene	1250	0.5	15.87	3	0.974
	1300	0.5	48.41	3	0.994
	1300	1.2	1.587	3	0.857
	1350	1.2	14.44	2	0.994
	1400	1.2	63.0	4	0.933
	1450	3.0	9.474	4	0.865
	1500	3.0	195.0	2	0.991
Orthopyroxene	1250	0.5	11.11	3	0.944
	1300	0.5	22.75	3	0.995
	1300	1.2	5.820	3	0.960
	1350	1.2	21.11	2	0.976
	1400	1.2	27.78	2	1
	1450	3.0	44.20	3	0.981
	1500	3.0	113.3	2	0.997
Spinel	1250	0.5	1.058	3	0.762
	1300	0.5	4.099	3	0.937
	1300	1.2	0.7508	4	0.338
	1350	1.2	1.058	3	0.762
	1400	1.2	2.889	4	0.751
	1450	3.0	6.053	4	0.964
	1500	3.0	55.74	3	0.998
Garnet	1300	1.2	290.5	3	0.900
	1400	1.2	1317.0	1	–
	1450	3.0	52.28	4	0.982
	1500	3.0	398.3	2	1.000

3.3. Thornber and Huebner (1985)

Thornber and Huebner (1985) studied olivine dissolution in melts of two different compositions (Ta-

Table 5
Summary of dissolution rates at 10^5 Pa extracted from experimental data of Thornber and Huebner (1985)

Mineral	T (°C)	dh/dt (10^{-7} cm s^{-1})	N	R^2
Olivine (Fo_{92})	1263	0.0579	1	–
	1265 [a]	0.1196	3	0.999
	1280	0.934	1	–
	1285	1.452	2	0.970
	1297	1.90	1	–
	1315	5.741	2	0.992
	1326	5.35	1	–
	1330	5.951	2	0.986
	1450	171.0	1	–
([b])	1240	0.284	1	–
([b])	1270	2.05	1	–
([b])	1284	2.42	1	–
([b])	1315	9.72	1	–

[a] Includes one experiment at 1266°C.
[b] Silica-enriched melt composition.

Table 6
Summary of dissolution rates extracted from experimental data of Zhang et al. (1989)

Mineral	T (°C)	P (GPa)	dh/dt (10^{-7} cm s^{-1})	N	R^2
Olivine [a]	1270	0.55	0.9727	1	–
	1285	0.55	4.796	1	–
	1290	0.55	2.688	2	0.976
	1365	1.3	30.90	1	–
	1375	1.5	57.22	1	–
	1400	0.55	27.92	1	–
Olivine (Fo_{100})	1305	0.55	3.059	2	0.543
Clinopyroxene	1305	1.05	10.40	2	0.871
	1365	1.3	30.93	1	–
	1375	2.15	79.78	1	–
Spinel	1385	1.3	7.865	1	–

[a] Olivine composition varies between Fo_{88} and Fo_{91}.

Table 7
Activation energies (kJ/oxygen equivalent moles) implied by fits to data shown in Figs. 3 and 4

Reference	Mineral	P (GPa)	Activation energy (kJ/o.e.m)
Donaldson (1985)	quartz	10^{-4}	180
	plagioclase ($An_{59.5}$)	10^{-4}	310
	plagioclase ($An_{29.5}$)	10^{-4}	210
	olivine ($Fo_{91.5}$)	10^{-4}	550
	olivine ($Fo_{88.5}$)	10^{-4}	650
Brearley and Scarfe (1986)	olivine	0.5	610
		1.2	360
		3.0	850
	clinopyroxene	0.5	440
		1.2	810
		3.0	1540
	orthopyroxene	0.5	280
		1.2	340
		3.0	480
	spinel	0.5	540
		1.2	290
		3.0	1130
	garnet	1.2	330
		3.0	1030
Zhang et al. (1989)	olivine [a]	0.55–1.5	590
	clinopyroxene [a]	1.05–2.15	1800
Thornber and Huebner (1985)	olivine	10^{-4}	870
	olivine [b]	10^{-4}	920

[a] In andesitic melt.
[b] In Si-enriched basaltic melt.

ble 2): lunar basalt #77115 and a silica-enriched variant of #77115 (Sil-77115). The experimental conditions and results are given in Table 5. They report a total of 25 isothermal, superliquidus dissolution experiments including 18 on the basalt and another 7 using the silica-enriched melt. All of their experiments use olivine (Fo_{92}) cut into crystallographically oriented rectangular parallelepipeds. Changes in thickness with time (dh/dt) were determined by measuring the thickness perpendicular to the largest surface area of the mineral plates before and after the experiments. Reported measurement errors are ± 0.0002 cm. The internal consistency of this dataset is not well-constrained because of the lack of repeated isothermal, isobaric experiments.

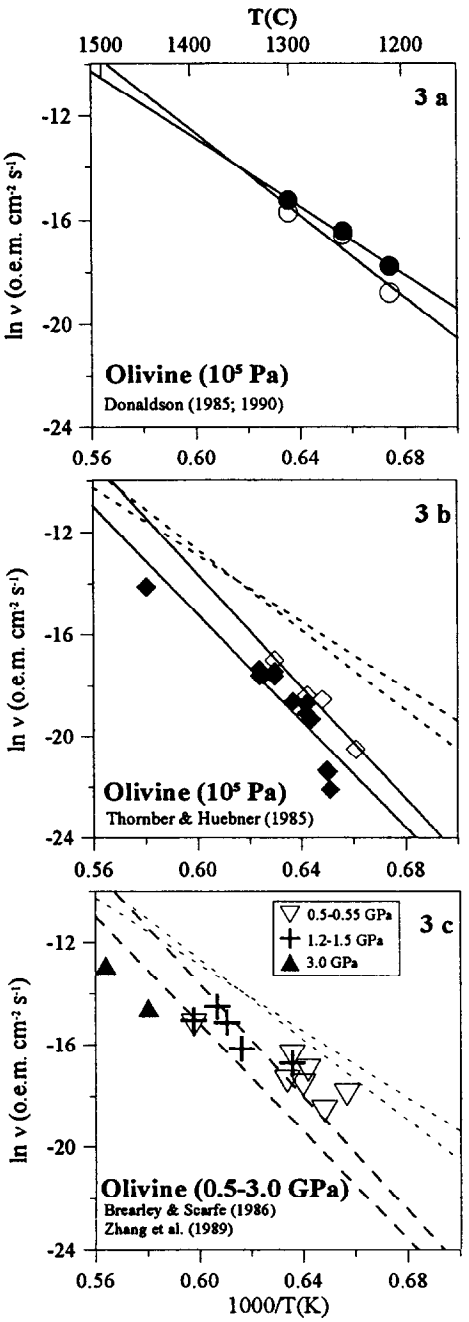

Fig. 3. Normalized experimentally- measured values of ν (oxygen equivalent moles (o.e.m.) cm^{-2} s^{-1}) for olivine are plotted as $\ln \nu$ vs. $1000/T$ (K) for: (a) 10^5 Pa data from Donaldson (1985) ($Fo_{88.5}$ = filled circles) and Donaldson (1990) ($Fo_{91.5}$ = open circles); (b) 10^5 Pa data from Thornber and Huebner (1985) for Fo_{92} (high Al basalt = filled diamonds, Si-enriched high Al basalt = open diamonds) shown against fits (dashed lines) to Donaldson (1985, 1990) data; (c) high P data (0.5–3.0 GPa) from Brearley and Scarfe (1986) and Zhang et al. (1989) compared to fits on 10^5 Pa experiments (dashed lines).

3.4. Zhang et al. (1989)

Zhang et al. (1989) used an andesitic melt (Table 2) to dissolve crystals of forsterite ($N = 3$), diopside ($N = 4$), quartz ($N = 1$), spinel ($N = 1$), rutile ($N = 1$), as well as natural San Carlos olivine ($N = 10$) over a range of T (1215–1400°C) and P (0.5–2.3.0 GPa) (Table 6). The starting crystals were cut and ground into cylinders to the exact diameter of the experimental charge, thereby isolating melt reservoirs on either side of the mineral. This dataset is similar to that of Thornber and Huebner (1985) in that few isothermal, isobaric experiments were repeated (3 out of 11) making it difficult to assess the internal consistency of the experiments.

3.5. Comparison of reported data for olivine

The experimental dataset for olivine is by far the largest and serves to illustrate the effects of mineral stability, T, and P on values of ν. Fig. 3a presents the datasets of Donaldson (1985, 1990) plotted as $\ln \nu$ (o.e.m. cm^{-2} s^{-1}) vs. $1000/T$ (K). The data, represented by solid circles ($Fo_{88.5}$) and open circles

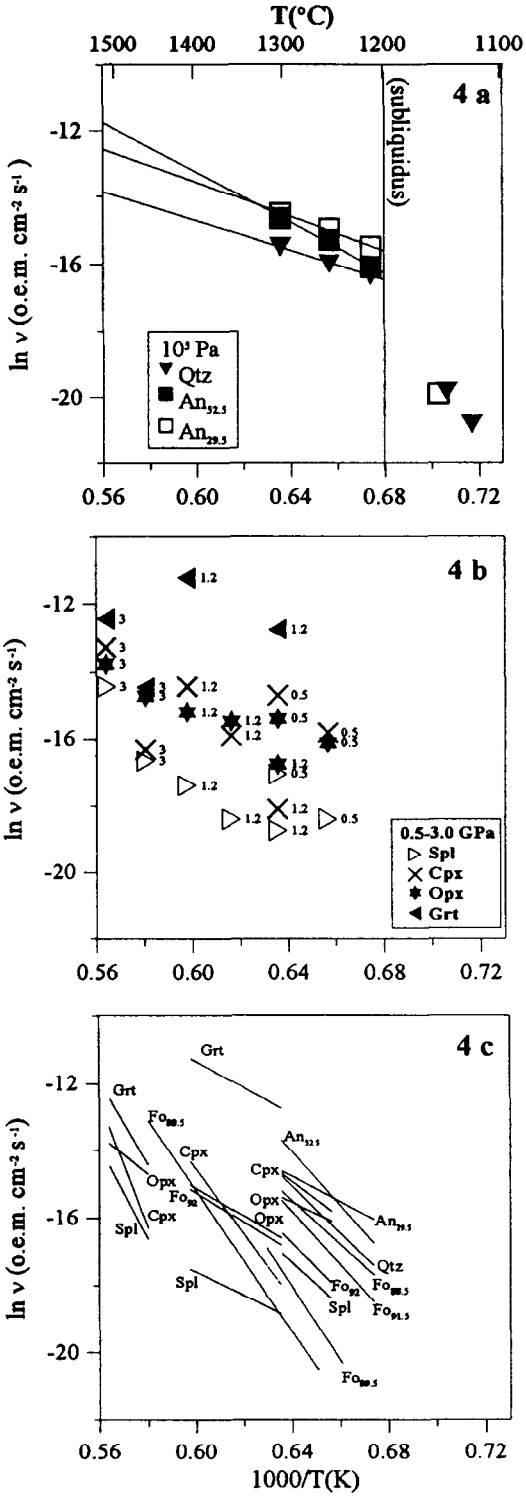

Fig. 4. Diagram summarizing $\ln v$ (measured) vs. $1000/T$ (K) relationships for: (a) 10^5 Pa data from Donaldson (1985) for quartz and plagioclase ($An_{29.5}$ and $An_{52.5}$); (b) higher P (0.5–3.0 GPa) data from Brearley and Scarfe (1986) for spinel, clinopyroxene, orthopyroxene and garnet (numbers by symbols denote values of P in GPa); and (c) all data in this database. The fits shown in (a) are based on superliquidus data only. The mineral abbreviations are: *Grt* = garnet, *Cpx* = clinopyroxene, *Opx* = orthopyroxene, *Spl* = spinel, *Qtz* = quartz, *Fo* = forsterite, *An* = anorthite.

($Fo_{91.5}$), demonstrate the small differences in values of v for slightly different olivine compositions dissolving in the same melt composition at the same values of T and P. These two datasets strongly support an Arrhenian relationship between v and T. Activation energies (E_A) are calculated from the slope of the best-fit line to the data divided by the gas constant and are reported in Table 7. Uncertainties in values of $\ln v$ which arise from variances in the isothermal experimental data (e.g., Fig. 1) are generally smaller than the symbol size in Figs. 3 and 4. A more complete treatment and discussion of error propagation is given in Appendix A.

Fig. 3b gives a summary of all the $P = 10^5$ Pa data for olivine dissolution in basaltic melts and consists of data from Donaldson (1985, 1990) (dashed lines) and Thornber and Huebner (1985) (solid lines and symbols). For both sets of polythermal experiments the data are Arrhenian. The olivine used by Thornber and Huebner (1985) dissolves at slower rates than those of Donaldson (1985, 1990), and the values of v are higher in the silica-enriched melt. Calculated values of E_A for the Thornber and Huebner (1985) data are ~300 kJ/o.e.m. higher than those for the Donaldson data (Table 7).

Fig. 3c shows data of the Brearley and Scarfe (1986) and Zhang et al. (1989) datasets for values of P ranging from 0.5 to 3.0 GPa. The values of $\ln v$ fall in a narrow band between the two sets of 10^5 Pa data from Donaldson (1985, 1990) and Thornber and Huebner (1985). The 0.5, 1.2, and 3.0 GPa experiments define trends with slopes subparallel to the 10^5 Pa experiments and have calculated values of E_A intermediate between the bounding sets of 10^5 Pa experiments (Table 7).

3.6. Comparison between all reported mineral dissolution data

The datasets available for other minerals are fewer in number than the dataset for olivine. Fig. 4a illustrates the Arrhenian behavior of quartz and plagioclase dissolution in basaltic melts at superliquidus temperatures and $P = 10^5$ Pa (Donaldson, 1985). The Arrhenian behavior of $\ln \nu$ is disrupted for quartz and one composition of plagioclase (An_{29}) below the liquidus T for the melt. For quartz, the break corresponds with crystallization of pigeonite around quartz during the experiment (Donaldson, 1985). Quartz has a smaller value of ν than either composition of plagioclase and has a lower calculated E_A than found for all other minerals in this study (Table 7).

Fig. 4b illustrates the absolute differences in values of ν for spinel, clinopyroxene, orthopyroxene, and garnet dissolving in a basaltic melt (Brearley and Scarfe, 1986). The values of $\ln\nu$ are Arrhenian and are given in Table 7. For all four minerals the calculated values of E_A increase between 0.5 to 3.0 GPa. Relative dissolution rates (ν) over the range of P (0.5–3.0 GPa) increase from spinel, to orthopyroxene ≅ clinopyroxene to garnet.

The $\ln \nu$ vs. $1000/T$ relationships for the entire group of minerals included in this compilation are presented in Fig. 4c. Over the range of values of T investigated, plagioclase and garnet have the highest values of ν while spinel and olivine have the lowest. The values of E_A are lowest for quartz, plagioclase, and garnet and highest for clinopyroxene and spinel (Table 7).

4. Discussion

4.1. Physicochemical controls on mineral dissolution

The data presented above allow us to evaluate the effects of time, T, P, and mineral composition on the calculated values of ν. As has been noted by previous workers (Donaldson, 1985; Thornber and Huebner, 1985; Brearley and Scarfe, 1986), the isothermal datasets have constant dissolution rates with respect to time (e.g., $d\nu/dt$ = constant). Dissolution rates that are time-independent imply that the mechanism controlling the process is also time-independent. Some workers have suggested that an interfacial mechanism is important in determining the rates of mineral dissolution (Wood and Walther, 1983; Thornber and Huebner, 1985), which would be a time-independent mechanism (Wood and Walther, 1983). Other workers have hypothesized that a time-dependent mechanism, such as diffusion of reactants to and from the mineral surface, is rate limiting (Cooper and Kingery, 1964; Kuo and Kirkpatrick, 1985a; Zhang et al., 1989). The data analyzed in this work do not support diffusion nor any other time-dependent mechanism as the rate-limiting step for mineral dissolution in basaltic silicate melts.

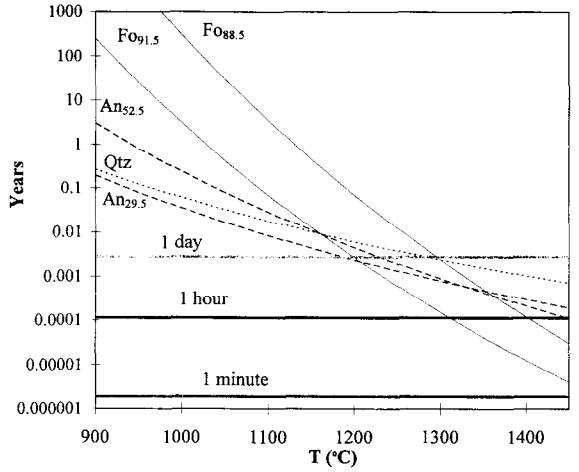

Fig. 5. Time (years) vs. T (°C) for complete dissolution of 1 cm diameter spheres of olivine ($Fo_{88.5}$ and $Fo_{91.5}$), plagioclase ($An_{52.5}$ and $An_{29.5}$), and quartz in a basaltic melt of constant composition at $P = 10^5$ Pa.

The values of ν systematically increase as a function of T for all of the minerals studied herein. Figs. 3 and 4 clearly establish the Arrhenius relationship between ν and $1/T$ (K); the strong Arrhenian behavior suggests the possibility of predicting values of ν as a function of T. Fig. 5 illustrates the importance of accurate and predictable dissolution rates for understanding the process of assimilation by silicate melts. Fig. 5 is a plot of years vs. T (°C) and maps the length of time required to completely dissolve a 1 cm diameter sphere of quartz, olivine, or plagioclase in a basaltic melt of constant composition at temperatures between 900° and 1450°C. Intervals of 1 min, 1 hr, and 1 day are marked for

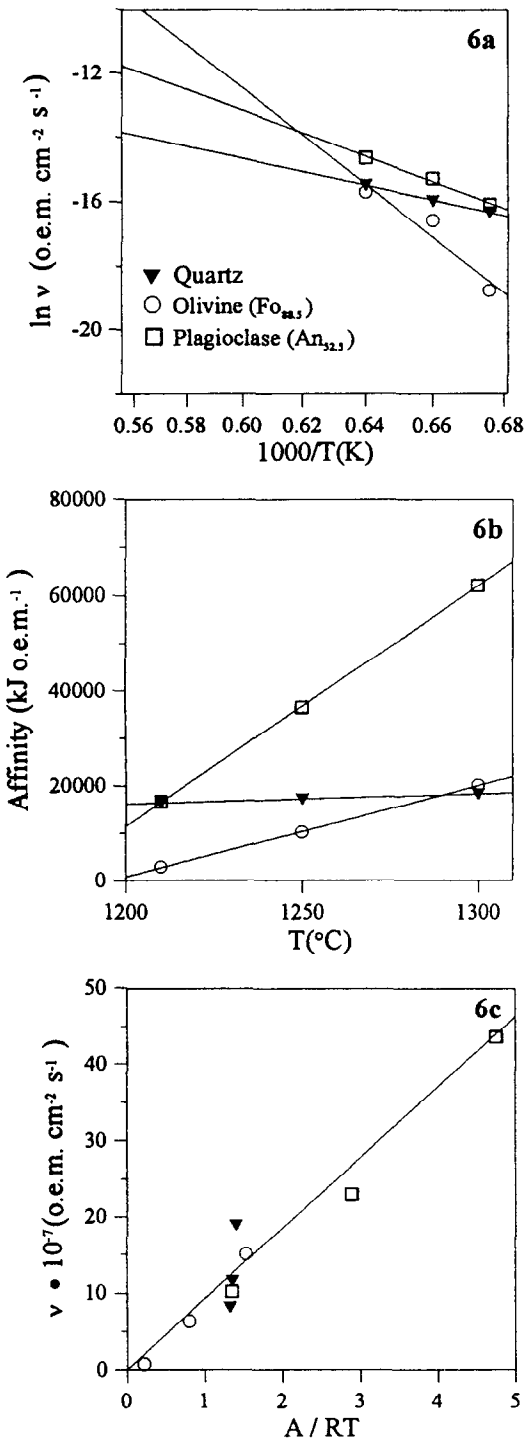

reference by heavy lines. Below 1300°C olivine ($Fo_{88.5}$) takes the most time to dissolve. For example, at 1200°C, plagioclase (An_{29}) would be completely dissolved in < 1 day and quartz would last ~ 3 days, whereas olivine ($Fo_{88.5}$) would take > 1 month to totally dissolve. However, above 1300°C quartz and plagioclase dissolve more slowly than either olivine composition.

For a xenolith comprising any combination of these minerals, the rate at which the minerals dissolve varies with temperature and is different for each of the minerals. The implications for the dynamics of chemical contamination of host melts based on non-uniform, T-dependent dissolution rates are very important.

The influence of P on the values of ν is not easy to evaluate with this database. For olivine (Fig. 3c), the high-pressure experiments of Brearley and Scarfe (1986) have values intermediate between the 10^5 Pa experiments of Donaldson (1985) and Thornber and Huebner (1985). However, based on differences for calculated values of E_A for clinopyroxene at 0.5 and 3.0 GPa (443 and 1535 kJ/o.e.m., respectively), increasing pressure appears to be an important variable controlling ν for some minerals.

4.2. Thermodynamic controls on mineral dissolution

Several workers have observed that relative rates of mineral dissolution for different mineral species are dependent on the relative thermodynamic stabilities of the minerals in the host melt (Kutolin and Agafonov, 1978; Scarfe et al., 1980; Kuo and Kirkpatrick, 1985a; Thornber and Huebner, 1985; Brearley and Scarfe, 1986). Brearley and Scarfe (1986) stated that "a significant factor in determining the mobility of species in the melt during a dissolution

Fig. 6. Relationships leading to predictive models for mineral dissolution in silicate melts illustrated with the 10^5 Pa experiments of Donaldson (1985): (a) $\ln \nu$ vs. $1000/T$ (K) for olivine, quartz, and plagioclase; (b) calculated A vs. T (°C) for olivine, quartz and plagioclase at superliquidus conditions; (c) $\nu \cdot 10^{-7}$ vs. calculated A/RT. Values of A are calculated using the MELTS software of Ghiorso and Sack (1995) and normalized to kJ/o.e.m.

process is the stability of the mineral'' (p.1177). The thermodynamic potential that best represents the degree of disequilibrium between a crystal and a melt or the stability of that phase at a specific P and T is the affinity (A) (Prigogine, 1967; Lasaga, 1981a; Aagaard and Helgeson, 1982; Ghiorso, 1987; Zhang et al., 1989). Values of A for a reaction are defined at constant T and P to be equal to the chemical potential of the reactant(s) minus the chemical potential of the product(s) (Prigogine, 1967). At equilibrium A is zero. Earlier workers were unable to quantify the 'relative' stabilities of the different minerals (Brearley and Scarfe, 1986) because they lacked a comprehensive thermodynamic database for mineral-melt equilibria. The new thermodynamic melt parameterization of Ghiorso and Sack (1995) provides a method for obtaining quantitative estimates of the thermodynamic properties of silicate melts and thereby allows us to calculate values of A for reactions between minerals and silicate melts.

Following the lead of workers investigating mineral dissolution in aqueous systems (e.g., Nagy et al., 1991), we have attempted to relate the dissolution rates presented above to the thermodynamic driving force for the dissolution reactions (Fig. 6). We have already shown that values of ν for the mineral dissolution experiments from Donaldson (1985) obey the Arrhenius relationship (Fig. 6a). We have calculated values of A for these mineral dissolution reactions using the melt composition, T and P of the experiments as input parameters for the MELTS software package (Ghiorso and Sack, 1995). Fig. 6b demonstrates the relationship between calculated A (normalized to o.e.m.) and T (°C). The methodology for calculating the values of A is explained in Appendix B. The experimentally derived values of ν show a linear relationship to calculated A/RT (K) (Fig. 6c). For values of $A/RT < 1$, irreversible thermodynamics predicts this linear relationship (Aagaard and Helgeson, 1982; Lasaga, 1981a,b). However, as discussed by Prigogine (1967, p.60), even where values of A for the net reaction (as opposed to the elementary reactions) are much greater than unity, the linear phenomenological relationship between A/RT and ν can still hold. Indeed, for the limited data presented in Fig. 6c, it appears that for these minerals in basaltic silicate melts the linear relationship holds.

5. Conclusions

Clearly, the study of mineral dissolution kinetics in silicate melts is still in its infancy. One observation from this study is that overall there is a paucity of data on the rates of dissolution for silicate minerals in natural silicate melt compositions. The published datasets are of variable quality, due mainly to incomplete descriptions of experimental conditions. In particular, information on sample geometries, measured sample dimensions and repeated isothermal experiments of different time-scales are critical. Notwithstanding the paucity of data, we can draw some important preliminary conclusions from this analysis. Mineral dissolution rates are Arrhenian for superliquidus conditions and for some minerals may be dependent on P as well. Preliminary calculations suggest that experimentally derived values of ν may have a systematic relationship to calculated values of A. We are currently working to include other datasets in our database and further explore the predictive potential of calculated A for assessing mineral dissolution in silicate melts.

Acknowledgements

Financial support for this research was funded in part by NSERC Research Grant OGP0820, an NSERC CRD Grant with Canamera Geological Ltd., and a University Graduate Fellowship from the University of British Columbia (to BRE). We are indebted to K.A. Felknor-Edwards for help with database editing. We thank J. Nicholls, G. Dipple, and K.J. Kirkpatrick for helpful discussions on thermodynamic modelling, data normalization and supplying unpublished data, respectively. Reviews by two anonymous reviewers, K. Arden and especially L. Stillings substantially improved the manuscript. All remaining inconsistencies are the responsibilities of the authors. (*SB*)

Appendix A. Error propagation

Least squares regression of the experimental data yields a slope (m) and an uncertainty on the slope (σ_m) that reflects how well the data fit a linear

model. This uncertainty can be propagated through subsequent calculational procedures used to compute ν. For example, to convert the nominal dissolution rate (ν^*) and its associated uncertainty (σ_{ν^*}) to the appropriate normalized dissolution rate (ν) and its associated uncertainty (σ_ν) given

$$\nu = f(\nu^*) \tag{A-1}$$

requires propagation of σ_{ν^*} through the following equation:

$$\sigma_\nu = \sqrt{(d\nu/d\nu^*)^2 \cdot \sigma_{\nu^*}^2} \tag{A-2}$$

For all rates reported in Tables 3–6 with values of $R^2 > 0.9$, the propagated errors are equal to or smaller than the symbol sizes in Figs. 3, 4, and 6a.

Appendix B. Calculation of chemical affinities

By definition, the affinity (A) for a reaction is equal to:

$$A = -\Sigma \alpha_i \mu_i \tag{B-1}$$

where α_i is the stoichiometric reaction coefficient and μ_i is the chemical potential of each of the components involved in the reaction (Prigogine, 1967). Thus, the value of A for the reaction $SiO_{2(Qtz)} \rightarrow SiO_{2(melt)}$ can be calculated using:

$$A = -\left[\alpha_{qtz}\left(\mu^\circ_{qtz} + RT \ln a_{SiO_2,qtz}\right) + \alpha_{SiO_2,liq}\left(\mu^\circ_{SiO_2,liq} + RT \ln a_{SiO_2,liq}\right)\right] \tag{B-2}$$

where a_{SiO_2} represents the activity of SiO_2 in quartz or the melt phase. The values of A for a given reaction are calculated using standard state thermodynamic properties for solids from Berman (1988) and the corresponding melt properties from Ghiorso and Sack (1995). Alternatively, the MELTS software (available from http://msgmac.geology.washington.edu/MeltsWWW/Melts.html) provides values of A for a limited set of mineral compositions at specified values of T, P and melt composition.

References

Aagaard, P. and Helgeson, H.C., 1982. Thermodynamic and kinetic constraints on reactions rates among minerals and aqueous solutions, I. Theoretical considerations. Am. J. Sci., 282: 237–285.

Berman, R.G., 1988. Internally-consistent thermodynamic data for minerals in the system Na_2O–K_2O–CaO–MgO–FeO–Fe_2O_3–Al_2O_3–SiO_2–TiO_2–H_2O–CO_2. J. Petrol., 29: 445–522.

Brearley, M. and Scarfe, C.M., 1986. Dissolution rates of upper mantle minerals in an alkali basalt melt at high pressure: an experimental study and implications of ultramafic xenolith survival. J. Petrol., 27: 1157–1182.

Cooper, A.R. and Kingery, W.D., 1964. Dissolution in ceramic systems, I. Molecular diffusion, natural convection, and forced convection studies of sapphire dissolution in calcium aluminum silicate. Am. Ceram. Soc. J., 47: 37–43.

Donaldson, C.H., 1985. The rates of dissolution of olivine, plagioclase and quartz in a basalt melt. Mineral. Mag., 49: 683–693.

Donaldson, C.H., 1990. Forsterite dissolution in superheated basaltic, andesitic and rhyolitic melts. Mineral. Mag., 54: 67–74.

Edwards, B.R. and Russell, J.K. 1994. Compilation and evaluation of experimental dissolution rates of silicate minerals in natural silicate melts with comparison to thermodynamic models. Eos (Trans. Am. Geophys. Union), 75: 704–705 (abstract).

Ghiorso, M.S., 1987. Chemical mass transfer in magmatic processes, III. Crystal growth, chemical diffusion and thermal diffusion in multicomponent silicate melts. Contrib. Mineral. Petrol., 96: 291–313.

Ghiorso, M.S. and Sack, R.O., 1995. Chemical mass transfer in magmatic processes, IV. A revised and internally consistent thermodynamic model for the interpolation and extrapolation of liquid–solid equilibria in magmatic systems at elevated temperatures and pressures. Contrib. Mineral. Petrol., 119: 197–212.

Harrison, T.M. and Watson, E.B., 1983. Kinetics of zircon dissolution and zirconium diffusion in granitic melts of variable water content. Contrib. Mineral. Petrol., 84: 66–67.

Harrison, T.M. and Watson, E.B., 1984. The behavior of apatite during crustal anatexis: equilibrium and kinetic considerations. Geochim. Cosmochim. Acta, 48: 1467–1477.

Kuo, L.-C., 1982. Kinetics of crystal dissolution in the system diopside–forsterite–silica. Ph.D. Thesis, University of Illinois at Urbana-Champaign, Urbana-Champaign, Ill., 124 pp. (unpublished)

Kuo, L.-C. and Kirkpatrick, R.J., 1985a. Kinetics of crystal dissolution in the system diopside–forsterite–silica. Am. J. Sci., 285: 51–90.

Kuo, L.-C. and Kirkpatrick, R.J., 1985b. Dissolution of mafic minerals and its implications for the ascent velocities of peridotite-bearing basaltic magmas. J. Geol., 93: 691–700.

Kutolin, V.A. and Agafonov, L.V., 1978. Composition of the upper mantle in light of the relative stability of ultrabasic nodules. Geol. Geofiz., 19: 3–13.

Lasaga, A.C., 1981a. Transition state theory. In: A.C. Lasaga and R.J. Kirkpatrick (Editors), Kinetics of Geochemical Processes. Mineral. Soc. Am., Rev. Mineral., 8: 135–169.

Lasaga, A.C., 1981b. Rate laws of chemical reactions. In: A.C. Lasaga and R.J. Kirkpatrick (Editors), Kinetics of Geochemical Processes. Mineral. Soc. Am., Rev. Mineral., 8: 1–68.

Marvin, U.B. and Walker, D., 1985. A transient heating event in

the history of a Highlands troctolite from Apollo 12 soil 12033. Proc. 15th Lunar and Planetary Science Conf., Part 2. J. Geophys. Res., 90: C421–C429.

Nagy, K.L., Blum, A.E. and Lasaga, A.C., 1991. Dissolution and precipitation kinetics of kaolinite at 80°C and pH 3: the dependence on solution saturation state. Am. J. Sci., 291: 649–686.

Prigogine, I., 1967. Introduction to Thermodynamics of Irreversible Processes. Wiley, New York, N.Y., 3rd ed., 147 pp.

Scarfe, C.M., Takahashi, E. and Yoder, H.S., 1980. Rates of dissolution of upper mantle minerals in an alkali-olivine basalt melt at high pressures. Carnegie Institute Washington Yearbook, 79: 290–296.

Thornber, C.R. and Huebner, J.S., 1985. Dissolution of olivine in basaltic liquids: experimental observations and applications. Am. Mineral., 70: 934–945.

Tsuchiyama, A., 1985. Dissolution kinetics of plagioclase in the melt of the system diopside–albite–anorthite, and the origin of dusty plagioclase in andesites. Contrib. Mineral. Petrol., 89: 1–16.

Walther, J.V. and Wood, B.J., 1984. Rate and mechanism in prograde metamorphism. Contrib. Mineral. Petrol., 88: 246–259.

Watson, E.B., 1982. Basalt contamination by continental crust: some experiments and models. Contrib. Mineral. Petrol., 80: 73–87.

Wood, B.J. and Walther, J.V., 1983. Rates of hydrothermal reactions. Science, 22: 413–415.

Zhang, Y., Walker, D. and Lesher, C.E., 1989. Diffusive crystal dissolution. Contrib. Mineral. Petrol., 102: 492–513.